applied sciences

MDPI

Review

Emerging Optical Techniques for the Diagnosis of Onychomycosis

Chrysoula Petrokilidou [1], Georgios Gaitanis [2], Ioannis D Bassukas [2], Aristea Velegraki [3,4], Edgar Guevara [5], Martha Z Vardaki [1] and Nikolaos Kourkoumelis [1,*]

1 Department of Medical Physics, School of Health Sciences, University of Ioannina, 45110 Ioannina, Greece; chrisa_pe@hotmail.com (C.P.); martha.vardaki@msl.ubc.ca (M.Z.V.)
2 Department of Skin & Venereal Diseases, School of Health Sciences, University of Ioannina, 45110 Ioannina, Greece; ggaitan@uoi.gr (G.G.); ibassuka@uoi.gr (I.D.B.)
3 Mycology Research Laboratory & UOA/HCPF Culture Collection, 15772 Athens, Greece; aveleg@med.uoa.gr
4 Biomedicine SA, 11526 Athens, Greece
5 CONACYT-Universidad Autónoma de San Luis Potosí, 78210 San Luis Potosí, Mexico; eguevara@conacyt.mx
* Correspondence: nkourkou@uoi.gr

Received: 14 February 2020; Accepted: 24 March 2020; Published: 29 March 2020

Abstract: Onychomycosis is the most prevalent nail infection. Although it is not a life-threatening condition, it impacts the quality of life for many patients and often imposes a challenging diagnostic problem. The causative agents are dermatophytes, yeasts and non-dermatophytic moulds. Accurate and early diagnosis, including the identification of the causative species, is the key factor for rational therapy. Still, early diagnosis is not optimal as the current gold standard for the differentiation of the infectious agents is culture-based approaches. On the other hand, noninvasive optical technologies may enable differential diagnosis of nail pathologies including onychomycosis. When light penetrates and propagates along the nail tissue, it interacts in different ways with the components of either infected or healthy nail segments, providing a wealth of diagnostic information upon escaping the tissue. This review aims to assess alternative optical techniques for the rapid diagnosis of onychomycosis with a potential to monitor therapeutic response or even identify the fungal agent non-invasively and in real time in a clinical setting.

Keywords: onychomycosis; nails; keratin; Raman spectroscopy; OCT; confocal microscopy

1. Introduction

Onychomycosis is a common, chronic, highly-relapsing fungal nail infection that affects primarily the toenails [1]. It can impact the structural integrity of the whole nail, the matrix, bed, and nail plate. Despite being a non-life-threatening condition, onychomycosis influences the patients' quality of life due to disfigurement and pain. Additionally, the relation to immunosuppression and other co-morbidities, like diabetes mellitus [2], upgrades onychomycosis to a significant medical condition rather than a mere aesthetic problem. Fungal infections represent almost 50% of all nail conditions [3] with a prevalence varying between 3% and 26% in different populations around the world (4.3% across Europe and North America) [4]. Principal causative agents of onychomycosis are the dermatophytes, particularly *Trichophyton rubrum*, followed by yeasts (predominantly *Candida* species). The dermatophytes are specialized pathogenic fungi that digest the hard keratin of nail tissues into short peptides and amino acids which are further assimilated by the fungi via selective membrane transporters, ultimately leading to brittle and damaged nails [5]. A main structural component of keratins are cysteine moieties which confer chemical stability and tissue rigidity through crosslinking of disulphide bonds. The

secreted proteolytic activity of dermatophytes is manifested by excreting large quantities of sulphite for cleaving those disulphide bridges. The modified proteins become accessible for further digestion by various endo- and exoproteases that reportedly act as virulence factors [6]. Non-dermatophytic moulds are also implicated in the pathogenesis in some cases. The global prevalence of onychomycosis is expected to increase further due to the ageing of the population and the rising numbers of predisposed individuals [7,8]. The gold standard for the diagnosis of onychomycosis involves direct microscopic evaluation of nail clippings and culture of nail samples in specialized media. Culture of tissue probes permits the identification of the causative organism and confirms its viability in situ [9]. However, it is time consuming—requiring about 3–4 weeks of incubation—and has lower sensitivity than microscopy [10]. Although direct microscopy is an inexpensive and widely available diagnostic technique, its sensitivity is highly operator-dependent [11]. Fungal chitin staining with calcofluor white can increase the overall sensitivity of the method. Histological investigation of nail plate samples after PAS staining is an alternative microscopic approach to the diagnosis of onychomycosis. Typically, these methods are less effective in identifying the culprit fungal pathogen at species level. More elaborate diagnostic alternatives for onychomycosis include the detection of dermatophyte DNA by PCR-based amplification [12] and an antibody-based immunochromatography strip method [13]. Recently, Gupta and Nakrieko [14] reported that culture was three to four times more likely to report false-negative results compared to PCR, highlighting the major setback of false-negative cultures. Finally, an additional challenge concerns the evaluation of treatment outcome and the follow up of patients for relapses. There is a need for the evaluation of objective criteria in order to increase the concordance between the clinical mycological assessment of affected nails (i.e., clinical cure) and the laboratory one (i.e., mycological clearance) [15].

Optical techniques play a central role in modern clinical diagnostics and optical instrumentations or prototypes are currently being used or tested in clinical settings to assess health conditions and treatment outcomes. Their main advantage is that they allow real-time visualization of tissues at high spatial resolution, being minimally or non-invasive, and optionally portable. Herein, the evidence from the application of three imaging and spectroscopic modalities, namely optical coherence tomography (OCT), confocal laser scanning microscopy (CLSM), and Raman spectroscopy (RS) for the evaluation of onychomycosis, is presented. While they have not been established as reference methods, these techniques offer several advantages, being rapid, non-destructive, non-invasive and with the capacity for in vivo application.

2. Spectroscopy

Raman Spectroscopy (RS)

Raman spectroscopy is an optical technique based on the inelastic light scattering resulting from molecular vibrations. Raman scattering is a two-photon event and involves the change in the polarizability of the molecule in relation to its vibrational energy. The incident photon exchanges energy with the molecule, creating an induced dipole moment. The radiation emitted by this induced dipole moment results in the observed Raman scattering. Distinct and chemical composition-specific bands in the Raman spectrum represent a so-called "molecular fingerprint" of the sample under study. RS of bioprobes provides ample physico-chemical information to allow for detailed analysis of tissue composition at molecular level, such as the investigation of human hard (hair and nails) and soft (stratum corneum, callus) keratins [16]. With minimal water interference RS is a non-invasive technique suitable for in vivo studies and has been successfully applied in bio-medical research, e.g., for the in situ diagnosis of malignancies [17]. However, it is limited by the laser-induced fluorescence of organic molecules and an overall low signal-to-noise ratio [18].

The cleavage of disulphide bonds is an essential step in the pathophysiology of onychomycosis, and therefore of central interest as a target Raman spectra profile for the identification of the infection. The intensities and the Raman shift of the Cα-Cβ-S-S′-C′β-C′α band imply the conformation of the

disulphide bridges. Cysteine residues appear at 450–590 cm^{-1} and 600–650 cm^{-1}, assigned to the S–S stretching mode and C–S stretching mode, respectively (Figure 1).

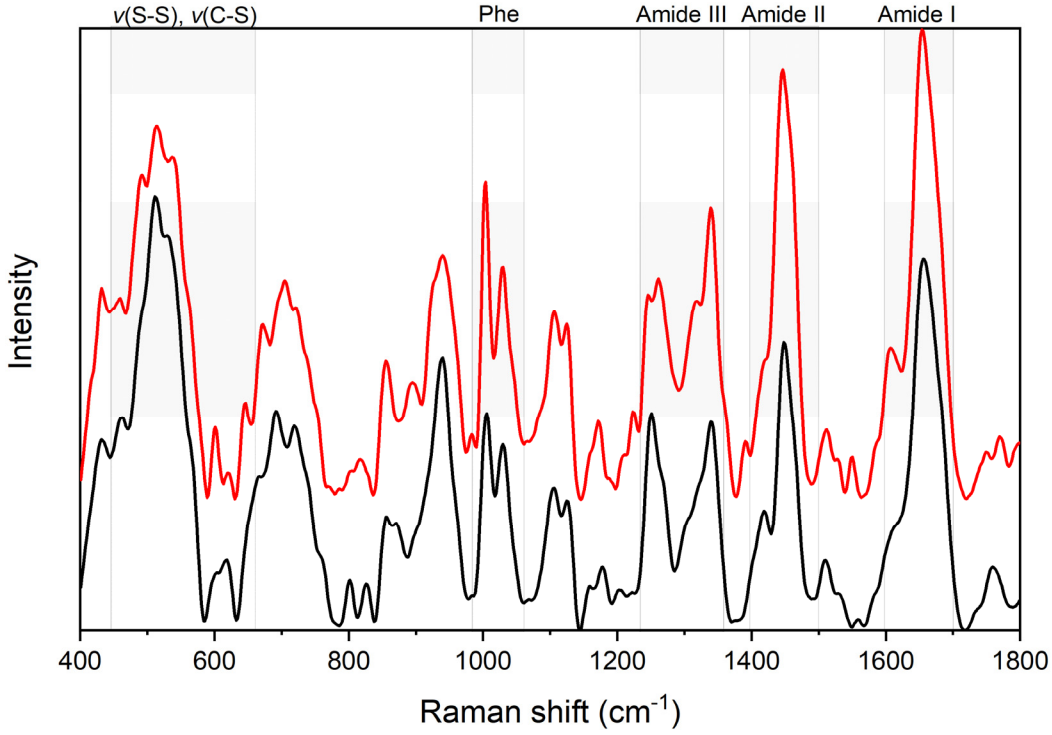

Figure 1. Raman spectra of nail clippings in the fingerprint region (400–1800 cm^{-1}); healthy (black), infected with *T. rubrum* (red). The spectra are vertically offset for clarity. Raman spectra were recorded using the i-Raman Plus portable Raman spectrometer (B&W Tek, Inc., Newark, DE, USA) with an excitation wavelength of 785 nm.

Cutrín-Gómez et al., [19] found a significantly lower ratio of peak areas of S–S to C–C bonds for onychomycotic compared to healthy nails, underlining the cleavage of the disulphide bridges. Moreover, a weak Raman peak at 2600 cm^{-1}, attributed to the S–H bond, was observed in diseased nails, further indicating the S–S bond break and the presence of the S–H moieties albeit in a lower proportion. On the contrary, Baraldi et al., [20] did not observe significant alterations of the S–S band in Raman spectra of onychomycosis nails. Moreover, they could not identify the S-H peak in either healthy or diseased nails. This vast discrepancy in the findings of the two groups may be, at least partly, attributed to differences in the methodological steps of the two studies, including dissimilar pre-processing (baseline correction) of the Raman spectra, different laser excitation wavelength, integration times, photothermal effects, sample storing temperature, etc. For example, the viability of the fungi is maintained in samples stored at 4 °C even though further growth, i.e., continuing keratin degradation, is inhibited [6].

Structural changes of nail keratin before and after treatment of onychomycosis with a neodymium-doped yttrium aluminium garnet (Nd:YAG) laser were also explored by Raman spectroscopy focusing on the impact on the disulphide band [21]. The effect of laser treatment on nail samples with onychomycosis was evaluated as a significant reduction in intensity and area of the disulphide band, by 55% and 38% respectively. Deconvolution of the disulphide band into two peaks assigned to gauche-gauche-gauche conformation (506 cm^{-1}) and the less stable gauche-gauche-trans conformation (518 cm^{-1}) [22] indicated destabilization of the S-S bond of the infected keratin structure after laser treatment. Previous RS studies on onychomycosis nail clippings [23] suggested that in healthy specimens the disulphide bond adopts the energetically more favorable gauche–gauche–gauche conformation, while in onychomycotic nail S–S Raman stretching modes

included additional contributions from the less stable gauche–gauche–trans conformation. It was also proposed that specimens from different patients had different S-S conformations, and the authors suggested that disulphide bond Raman density and shift might reflect the pathological level of severity and/or infection phase. However, since no identification of the causative organism at the species level was performed, we argue that variations of the S-S bond conformation can be pathogen-specific. To that end, Kourkoumelis et al., [24] performed RS measurements on 52 mycologically-characterized nail clippings in order to differentiate between healthy and either *T. rubrum* or *Candida* infected nails. In uninfected nails, the energetically stable gauche-gauche-gauche conformation was observed at 513–515 cm^{-1}. However, in samples infected with *Candida* species, a secondary shoulder at 519 cm^{-1} was observed, indicating the presence of the less stable gauche-gauche-trans conformation as well as the heterogeneity of the S-S bonds conformation among nails infected by different species. Likewise, Raman spectra of nails infected by *T. rubrum* featured two weak but well-defined bands at 619 cm^{-1} and 648 cm^{-1}, attributed to the C-S stretching vibration, that were not observed in either healthy or *Candida*-infected nails. Principal component analysis (PCA) successfully clustered specimens by species, and the corresponding loadings indicated that the bands responsible for the separation were assigned to the disulphide bridges. Subsequent classification of the RS spectra test set, using the soft independent modeling of class analogy (SIMCA) method, yielded 92.8% accuracy in discriminating between the three classes (healthy, *T. rubrum*- and *Candida*-infected nails) and 100% accuracy in classifying healthy vs onychomycotic nails.

These findings indicate that species-specific differences in fungal invasion mechanisms might trigger diverse chemical alterations of the nail plate, which can be reflected in the acquired Raman spectra and could be explored to differentiate among the culprit species of onychomycosis at patient-level in vivo. Dermatophytes, like *T. rubrum*, employ extracellular proteases (keratinases) which, together with the secretion of sulphite as a reducing agent [25], digest S-S bonds in order to assimilate degraded keratin moieties as a protein source [26]. Similarly, *Candida* species make use of extracellular enzymes with keratinolytic activity [27] to disrupt the S-S cross-linking of keratin, and in addition they excrete sulfite when confronted with elevated cysteine concentrations [28]. Moreover, in an ex vivo onychomycosis model (infection of nail clippings), RS was explored to differentiate between *Trichophyton* dermatophytic fungi (*T. rubrum*, *T. mentagrophytes* and *T. tonsurans*) and the non-dermatophytic species *S. brevicaulis* and *C. albicans* [29]. A correlation matrix approach was used to generate a dendrogram which visually illustrated the cluster arrangements, representing the dermatophytic in one cluster and the non-dermatophytic/yeast nail infections in a separate one. The 500–640 cm^{-1} spectral region was found to be the most promising discriminating factor since cysteine S–S and C-S bonds act as a correlate of nail rigidity and hardness. These bonds imply a densely-packed, folded structure of keratin with multiple S-S cross-linking and gauche-gauche-gauche conformation.

Other vibrational bands observed in Raman spectra of nail keratin are: (i) the phenylalanine (Phe) bands assigned to the symmetric ring breathing mode (1004 cm^{-1}) and C–H in-plane bending mode (1030 cm^{-1}); (ii) the amide I broad band (~1655 cm^{-1}) with major components' contribution from α-helix C = O stretching (~1652 cm^{-1}) and β-sheet C = O stretching (~1670 cm^{-1}); (iii) the amide II band (~1450 cm^{-1}) assigned to the deformation of –CH, $–CH_2$ and $–CH_3$; and (iv) the amide III broad band (~1350 cm^{-1}) attributed to C–N stretching and $–CH_2$ deformation and scissoring [24]. In onychomycotic nails, the ratio of the peak area of the α-helical band divided by the peak area of the β-sheet was found to be lower than the corresponding value in normal nails [23]. The secondary structure of α-keratin forms coiled-coil domains that unravel under onychomycosis, inducing a less dense coil-loose protein structure. Nevertheless, this finding seems to be inconsistent and possibly specific to a causative agent. Finally, it is worth noting that in Nd:YAG laser-treated nails, the β-sheet band dominated over the α-helical structures, contrary to the outcomes for the non-treated onychomycotic nails [21].

3. Imaging Techniques

3.1. Optical Coherence Tomography (OCT)

OCT is a non-invasive technique for real-time cross-sectional imaging of living tissues on the micron scale, based on the interferometric measurement of the echo time delay and the magnitude of a back-scattered low-power infrared laser light beam. Light emitted from the source is divided into two beams which are then combined to produce an interference signal. One beam is directed to the tissue sample and reflected by the internal structure, while the other hits a reference mirror. By adjusting the path length of the reference beam, the signal amplitude can be calculated as a function of the depth in the tissue [30,31]. The ballistic (back-scattered) and near-ballistic (back-reflected) photons give the depth information during image reconstruction [32]. This back-scattered intensity constitutes what is usually called an A-line, depicted in Figure 2a. In order to generate a B-scan or two-dimensional scan (panel (b) of Figure 2), several axial scans (A-lines) are obtained at different transverse locations. Finally, by shifting a series of B-scans, a three-dimensional dataset can be achieved, as depicted in Figure 2c.

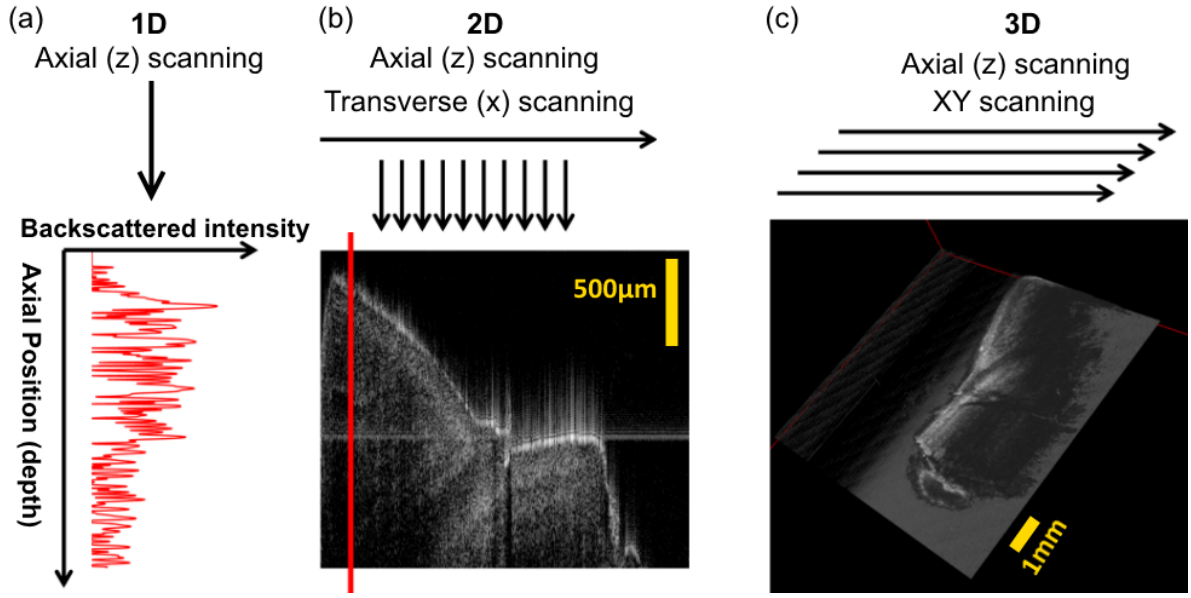

Figure 2. Diagram depicting the formation of a tomographic OCT image of a healthy nail and fingertip. (**a**) A-line or axial scan, (**b**) bidimensional scan or B-scan and (**c**) volumetric scan. Custom-built OCT based on Axsun swept-source laser (Axsun, 1310 Swept Source Engine, MA, USA). Reproduced from [33].

OCT imaging has the potential to discriminate elusive alterations in the nail unit for early detection and diagnosis of fungal infections. Furthermore, being non-invasive, time series analysis of a single sample can be applied to evaluate therapeutic interventions. OCT scans last only a few seconds and since the instrument sends low power density infrared light to the nail (optical window 700–1500 nm) it causes no discomfort to the patient. Moreover, multiple locations of the same nail plate can be screened in parallel.

OCT is currently employed in studies as a clinical diagnostic tool for nail disorders. Due to the high spatial resolution, OCT can detect subtle morphological changes to healthy nail units with a higher sensitivity compared to high-frequency ultrasound, demonstrating a clear separation of the nail bed from the nail plate. OCT images clearly showed the layered structure of the nail, the morphological components of the epidermis and the upper dermis, and the area of the nail matrix below the proximal nail plate, along with accurate measurements of the thickness of the nail plate [34]. Onychomycosis is

depicted in OCT scans as longitudinal hyper-reflective lines within the nail plate. These linear OCT structures seem to correspond to high scattering "tunnels" or small "cleavage levels" that penetrate the nail plate from the surface inwards and are surrounded by relatively low scattering areas. The structures in Figure 3 correspond to the presence of fungal elements which, due to their high chitin content, reflect light stronger than the surrounding nail components [35].

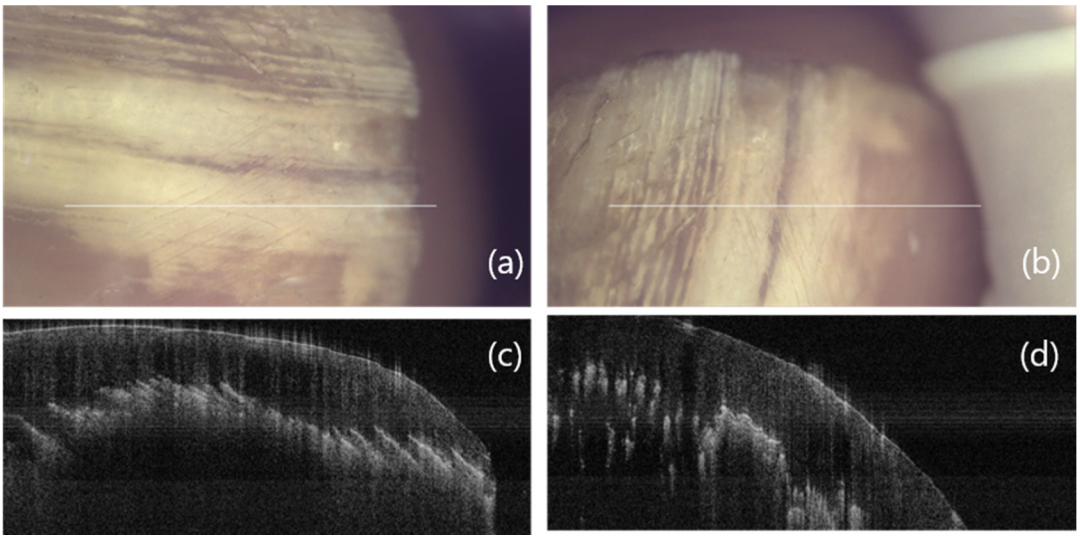

Figure 3. Optical and OCT images of nail infected by *T. rubrum* (culture-confirmed by direct KOH microscopy). The white line (9 mm) in the clinical picture (**a**,**b**) indicates the vertical plane that the OCT image was taken at (**c**,**d**). The multiple hyper-reflective, poorly defined, wisp-like streaks seem to originate from the hyponychium towards the nail plate at oblique angles relative to the nail's surface, as if the fungal hyphae move towards undigested keratin (chemotaxis). Images were acquired with NITID OCT (DermaLumics, Madrid, Spain).

In addition, infected nails may show a non-uniform layering under the nail plate, a rather sharp transition from the nail plate to nail bed and a 70% thickening of the infected nail [36]. Furthermore, signal shadows due to the increased surface irregularity with inclined lines and spots of higher reflectance capacity were observed, contrary to healthy nails which appeared as homogeneous band-like structures with varying degrees of signal intensity and thickness and an obvious separation of the nail bed [37].

Besides nail plate infection, the identification of morphological attributes of a dermatophytoma, a feature negatively impacting the efficacy of onychomycosis treatments, was also described with OCT [38]. Dermatophytoma was depicted as a clearly demarcated hyper-reflective homogenous accumulation beneath an inhomogeneous nail plate. The hyper-reflective area was shown to correspond to the characteristics of the dermatophytoma "fungal ball", at a depth of 0.55 to 0.98 mm below the nail plate. Moreover, cuticula and proximal fold were depicted as highly scattering structures in contrast to the low scattering matrix.

Finally, compared to established diagnostic procedures for onychomycosis, OCT seems to be more reliable than KOH preparation and nail clippings culture which are both susceptible to type II (false negative) errors [35]. From a methodological point of view, the OCT approach to onychomycotic nail plate diagnosis can be compared to the histopathological screening of nail plate serial sections for the presence of hyphae. Cross-correlation with histology showed that in onychomycotic nails high-scattering structures are conglomerates of hyphae [35]. However, with OCT there is no need for nail plate sampling and an almost indefinite number of vertical sections are available for subsequent evaluation. Yet a distinct limitation of OCT is the fact that alterations in the hyponychium and the surface of the nail plate cannot be evaluated with the same efficacy as the nail plate. Nevertheless, in a

prospective trial on 50 patients with suspected onychomycosis [39], OCT had the lowest specificity of 42.9%. Moreover, OCT had negative predictive value of 75%, higher than CLSM (68%), histopathology (63.6%) and culture (40.4%), but lower than PCR (91.3%). Both positive (i.e., the probability that nails with positive screenings are indeed affected by onychomycosis) and negative (i.e., the probability that nails with negative results are indeed not affected by onychomycosis) predictive values of OCT were 75%. The high number of false positive outcomes was attributed to the OCT's inherent inability to differentiate between hyphae or fungal spores within the nail plate and structural artefacts (e.g., trapped air) that add image noise to the optical signal.

3.2. Confocal Laser Scanning Microscopy (CLSM)

CLSM is a complementary technique to conventional microscopy with increased resolution towards ultrastructural details. In conventional microscopy, the image quality may be seriously undermined by artefacts originating from specimen fixation and sectioning [40]. CLSM offers high-resolution images with a lateral resolution down to 140 nm and axial resolution of 1 mm, offering the visualization of the tissue in consecutive sections parallel to the surface of the sample. CLSM is a light reflection technique based on a spatial filter to block out-of-focus light. While light is illuminating the sample, a confocal microscope focuses a beam at one narrow depth level each time, achieving highly-confined depth of focus, effectively suppressing light from out-of-focus planes and reconstructing the image in x/y/z-directions [41].

CLSM images of healthy fingernails reveal a three-zonal "sandwich" nail structure consisting of a brighter uppermost surface-reflection layer, followed by a layer with poorer signal and finally a brighter deeper zone (Figure 4). The nail bed is demonstrated as a wave structure, however, only in relatively thinner nails (<500 μm) [42]. Single corneocytes can be visualized within the healthy nail plate while hyphae of dermatophytes were observed in onychomycotic nails [37]. Moreover, direct fungal quantification can be performed by analyzing the location and the density of the fungi [43].

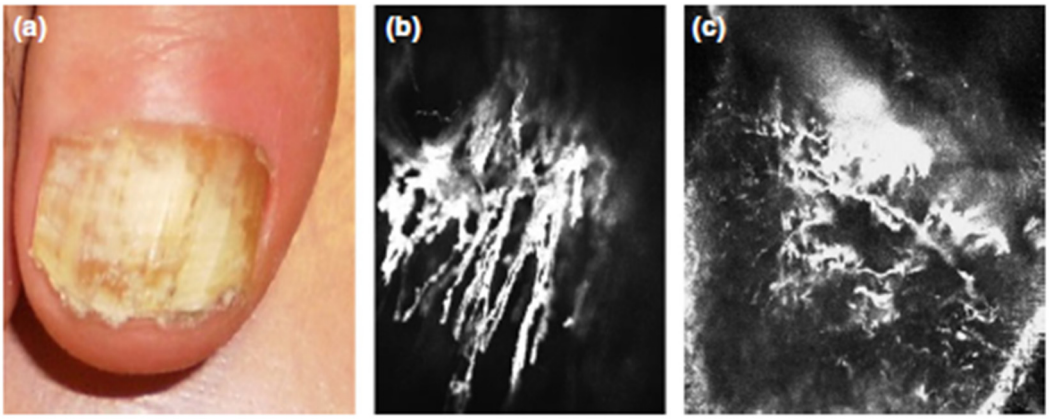

Figure 4. Images of onychomycotic nail: (**a**) Clinical, (**b**) in vivo CLSM and (**c**) ex vivo CLSM. The hyper-reflective, branching, linear structures are typical of fungal hyphae. Reproduced with permission from [42].

In vivo and in vitro confocal infrared microscopy, exploiting a 1064 nm Nd:YAG laser, revealed the presence of branched hyphae in both onychomycotic toenails of a patient [44]. Pharaon et al., [45] examined 58 patients with clinical suspicion of distal and lateral subungual onychomycosis covering 10–75% of the surface of at least one great toenail by reflectance confocal microscopy (RCM). Onychomycosis was characterized by the presence of bright filamentous branching structures corresponding to hyphae on at least three consecutive images. RCM classified correctly 79.3% of the onychomycotic samples with 52.9% sensitivity and 90.2% specificity. Moreover, CLSM can detect the location and density of the pathogen but it cannot discriminate between dermatophytes and non-dermatophytic moulds or yeasts [46].

A detailed analysis of the performance of CLSM as diagnostic tool for onychomycosis was reported by Rothmund et al. [39]. In a prospective trial, 50 patients with suspected onychomycosis and 10 controls were cross-examined with CLSM in comparison to three reference techniques (PCR, fungal culture and PAS staining). CLSM showed the highest positive predictive value (88.6%) which was similar to KOH preparation (85.3%). The specificity of CLSM (81%) was superior to KOH preparation (76.2%) but inferior to PAS staining (100%). Moreover, CLSM (79.5%) exhibited a higher sensitivity to histopathology (69.2%) and KOH preparation (74.4%). Overall, although CLSM can principally aid the diagnosis of onychomycosis, it remains too sophisticated and expensive a technique to adopt for routine use in dermatological practice [47].

4. Conclusions

Onychomycosis is not just a cosmetic nuisance but a disorder with a reservoir of pathogenic fungi that can give rise to significant health problems. The standard clinical diagnostic algorithm of onychomycosis involves clinical suspicion and a positive laboratory test. Since the clinical presentation is not always conclusive, additional spectroscopic and imaging techniques are needed to aid the on-site diagnostic accuracy in a rapid and non-invasive manner. Proper diagnosis of onychomycosis is important for a rational treatment. The standard therapeutic approach involves the administration of systemic antifungal agents over a long period; for toenails, it typically exceeds 3 months. Thus, the confirmation of diagnosis, i.e., the definite identification of the fungal cause, is essential to protect patients from redundant and costly treatments. RS, OCT, and CLSM are well established modalities for the evaluation of skin diseases, and are currently also emerging as approaches to the study of nail infections. The chemical composition and the structural aspects of healthy and onychomycotic nails can be rapidly assessed using these methods. RS can be easily integrated into the clinical setting for real-time evaluation of onychomycosis. In particular, when RS is coupled with statistical methods, it can achieve flawless classification between healthy and onychomycotic nails, although the detailed discrimination of the different pathogens at species- or strain-level with the currently available instrumentation seems unlikely. OCT can identify morphological nail alterations indicative of onychomycosis, distinguish areas of infected nail and identify the depth of pathogen's invasion. However, it does not allow the differentiation between hyphae/spores and other nail creases and lacks specificity. CLSM takes advantage of its higher resolution, which allows for the detection of cellular and architectural abnormalities of the nail, can quantify the fungi load and has superior specificity compared to KOH preparation. As yet, species differentiation and vitality cannot be assessed with CLSM while it remains an expensive instrumentation. It is worth noting that the integration of different currently available techniques, with their different pros and cons, in a so-called multi-modality imaging approach, is anticipated to significantly improve our diagnostic capabilities in assessing onychomycosis by (i) rapidly identifying the fungal agent, (ii) monitoring treatment response, and (iii) evaluating therapeutic protocols.

Author Contributions: Conceptualization, C.P., G.G., and N.K.; methodology, G.G., I.D.B., A.V., and N.K.; investigation, C.P., E.G., M.Z.V., and N.K.; validation, all authors; writing—original draft preparation, N.K; writing—review and editing, all authors; supervision, N.K. All authors read and agreed to the published version of the manuscript.

Funding: This research received no external funding.

Acknowledgments: We thank Stavros Niarchos Foundation for the generous donation of the OCT device. E.G. would like to acknowledge the financial support provided by Cátedras CONACYT (project 528).

Conflicts of Interest: The authors declare no conflict of interest.

References

1. Bang, C.H.; Yoon, J.W.; Lee, H.J.; Lee, J.Y.; Park, Y.M.; Lee, S.J.; Lee, J.H. Evaluation of relationships between onychomycosis and vascular diseases using sequential pattern mining. *Sci. Rep.* **2018**, *8*, 17840. [CrossRef]

2. Elewski, B.E. Onychomycosis: Pathogenesis, Diagnosis, and Management. *Clin. Microbiol. Rev.* **1998**, *11*, 415–429. [CrossRef]
3. Faergemann, J.; Baran, R. Epidemiology, clinical presentation and diagnosis of onychomycosis. *Br. J. Dermatol.* **2003**, *149*, 1–4. [CrossRef] [PubMed]
4. Sigurgeirsson, B.; Baran, R. The prevalence of onychomycosis in the global population—A literature study. *J. Eur. Acad. Dermatol. Venereol.* **2014**, *28*, 1480–1491. [CrossRef]
5. Monod, M. Secreted proteases from dermatophytes. *Mycopathologia* **2008**, *166*, 285–294. [CrossRef] [PubMed]
6. Sharma, A.; Chandra, S.; Sharma, M. Difference in keratinase activity of dermatophytes at different environmental conditions is an attribute of adaptation to parasitism. *Mycoses* **2012**, *55*, 410–415. [CrossRef] [PubMed]
7. Scher, R.K.; Tosti, A.; Joseph, W.S.; Vlahovic, T.C.; Plasencia, J.; Markinson, B.C.; Pariser, D.M. Onychomycosis diagnosis and management: Perspectives from a joint dermatology-podiatry roundtable. *J. Drugs Derm JDD* **2015**, *14*, 1016–1021.
8. Jacobsen, A.A.; Tosti, A. Predisposing factors for onychomycosis. In *Onychomycosis*; Springer: Berlin/Heidelberg, Germany, 2017; pp. 11–19.
9. Ghannoum, M.; Mukherjee, P.; Isham, N.; Markinson, B.; Rosso, J.D.; Leal, L. Examining the importance of laboratory and diagnostic testing when treating and diagnosing onychomycosis. *Int. J. Dermatol.* **2018**, *57*, 131–138. [CrossRef]
10. Jung, M.Y.; Shim, J.H.; Lee, J.H.; Lee, J.H.; Yang, J.M.; Lee, D.-Y.; Jang, K.-T.; Lee, N.Y.; Lee, J.-H.; Park, J.-H.; et al. Comparison of diagnostic methods for onychomycosis, and proposal of a diagnostic algorithm. *Clin. Exp. Dermatol.* **2015**, *40*, 479–484. [CrossRef]
11. Weinberg, J.M.; Koestenblatt, E.K.; Tutrone, W.D.; Tishler, H.R.; Najarian, L. Comparison of diagnostic methods in the evaluation of onychomycosis. *J. Am. Acad. Dermatol.* **2003**, *49*, 193–197. [CrossRef]
12. Arabatzis, M.; Bruijnesteijn van Coppenraet, L.E.S.; Kuijper, E.J.; de Hoog, G.S.; Lavrijsen, A.P.M.; Templeton, K.; van der Raaij-Helmer, E.M.H.; Velegraki, A.; Gräser, Y.; Summerbell, R.C. Diagnosis of common dermatophyte infections by a novel multiplex real-time polymerase chain reaction detection/identification scheme. *Br. J. Dermatol.* **2007**, *157*, 681–689. [CrossRef] [PubMed]
13. Tsunemi, Y.; Hiruma, M. Clinical study of Dermatophyte Test Strip, an immunochromatographic method, to detect tinea unguium dermatophytes. *J. Dermatol.* **2016**, *43*, 1417–1423. [CrossRef] [PubMed]
14. Gupta, A.K.; Nakrieko, K.-A. Onychomycosis Infections: Do Polymerase Chain Reaction and Culture Reports Agree? *J. Am. Podiatr. Med. Assoc.* **2017**, *107*, 280–286. [CrossRef] [PubMed]
15. Werschler, W.P.; Bondar, G.; Armstrong, D. Assessing Treatment Outcomes in Toenail Onychomycosis Clinical Trials. *Am. J. Clin. Dermatol.* **2004**, *5*, 145–152. [CrossRef] [PubMed]
16. Williams, A.C.; Edwards, H.G.M.; Barry, B.W. Raman spectra of human keratotic biopolymers: Skin, callus, hair and nail. *J. Raman Spectrosc.* **1994**, *25*, 95–98. [CrossRef]
17. Kourkoumelis, N.; Balatsoukas, I.; Moulia, V.; Elka, A.; Gaitanis, G.; Bassukas, I. Advances in the in Vivo Raman Spectroscopy of Malignant Skin Tumors Using Portable Instrumentation. *IJMS* **2015**, *16*, 14554–14570. [CrossRef]
18. Kourkoumelis, N.; Polymeros, A.; Tzaphlidou, M. Background Estimation of Biomedical Raman Spectra Using a Geometric Approach. *Spectrosc. Int. J.* **2012**, *27*, 441–447. [CrossRef]
19. Cutrín Gómez, E.; Anguiano Igea, S.; Delgado-Charro, M.B.; Gómez Amoza, J.L.; Otero Espinar, F.J. Microstructural alterations in the onychomycotic and psoriatic nail: Relevance in drug delivery. *Eur. J. Pharm. Biopharm.* **2018**, *128*, 48–56. [CrossRef]
20. Baraldi, A.; Jones, S.A.; Guesné, S.; Traynor, M.J.; McAuley, W.J.; Brown, M.B.; Murdan, S. Human Nail Plate Modifications Induced by Onychomycosis: Implications for Topical Therapy. *Pharm. Res.* **2015**, *32*, 1626–1633. [CrossRef]
21. Shin, M.K.; Kim, T.I.; Kim, W.S.; Park, H.-K.; Kim, K.S. Changes in nail keratin observed by Raman spectroscopy after Nd:YAG laser treatment. *Microsc. Res. Tech.* **2017**, *80*, 338–343. [CrossRef]
22. Gniadecka, M.; Nielsen, O.F.; Christensen, D.H.; Wulf, H.C. Structure of Water, Proteins, and Lipids in Intact Human Skin, Hair, and Nail. *J. Investig. Dermatol.* **1998**, *110*, 393–398. [CrossRef] [PubMed]
23. Wen, W.; Meng, Y.; Xiao, J.; Zhang, P.; Zhang, H. Comparative study on keratin structural changes in onychomycosis and normal human finger nail specimens by Raman spectroscopy. *J. Mol. Struct.* **2013**, *1038*, 35–39. [CrossRef]

24. Kourkoumelis, N.; Gaitanis, G.; Velegraki, A.; Bassukas, I.D. Nail Raman spectroscopy: A promising method for the diagnosis of onychomycosis. An ex vivo pilot study. *Med. Mycol.* **2018**, *56*, 551–558. [CrossRef] [PubMed]
25. Grumbt, M.; Monod, M.; Yamada, T.; Hertweck, C.; Kunert, J.; Staib, P. Keratin Degradation by Dermatophytes Relies on Cysteine Dioxygenase and a Sulfite Efflux Pump. *J. Investig. Dermatol.* **2013**, *133*, 1550–1555. [CrossRef] [PubMed]
26. Léchenne, B.; Reichard, U.; Zaugg, C.; Fratti, M.; Kunert, J.; Boulat, O.; Monod, M. Sulphite efflux pumps in Aspergillus fumigatus and dermatophytes. *Microbiology* **2007**, *153*, 905–913. [CrossRef] [PubMed]
27. Vermelho, A.B.; Mazotto, A.M.; de Melo, A.C.N.; Vieira, F.H.C.; Duarte, T.R.; Macrae, A.; Nishikawa, M.M.; da Silva Bon, E.P. Identification of a Candida parapsilosis Strain Producing Extracellular Serine Peptidase with Keratinolytic Activity. *Mycopathologia* **2010**, *169*, 57–65. [CrossRef] [PubMed]
28. Hennicke, F.; Grumbt, M.; Lermann, U.; Ueberschaar, N.; Palige, K.; Böttcher, B.; Jacobsen, I.D.; Staib, C.; Morschhäuser, J.; Monod, M.; et al. Factors Supporting Cysteine Tolerance and Sulfite Production in Candida albicans. *Eukaryot. Cell* **2013**, *12*, 604–613. [CrossRef] [PubMed]
29. Smijs, T.G.; Jachtenberg, J.W.; Pavel, S.; Bakker-Schut, T.C.; Willemse-Erix, D.; de Haas, E.R.M.; Sterenborg, H. Detection and differentiation of causative organisms of onychomycosis in an *ex vivo* nail model by means of Raman spectroscopy. *J. Eur. Acad. Dermatol. Venereol.* **2014**, *28*, 1492–1499. [CrossRef]
30. Olsen, J.; Holmes, J.; Jemec, G.B.E. Advances in optical coherence tomography in dermatology—A review. *J. Biomed. Opt.* **2018**, *23*, 1. [CrossRef]
31. Huang, D.; Swanson, E.A.; Lin, C.P.; Schuman, J.S.; Stinson, W.G.; Chang, W.; Hee, M.R.; Flotte, T.; Gregory, K.; Puliafito, C.A.; et al. Optical coherence tomography. *Science* **1991**, *254*, 1178–1181. [CrossRef]
32. Gambichler, T.; Jaedicke, V.; Terras, S. Optical coherence tomography in dermatology: Technical and clinical aspects. *Arch. Dermatol. Res.* **2011**, *303*, 457–473. [CrossRef] [PubMed]
33. Guevara, E. Functional Connectivity of the Rodent Brain Using Optical Imaging. Ph.D. Thesis, École Polytechnique de Montréal, Montréal, QC, Canada, 2013. [CrossRef]
34. Mogensen, M.; Thomsen, J.B.; Skovgaard, L.T.; Jemec, G.B.E. Nail thickness measurements using optical coherence tomography and 20-MHz ultrasonography. *Br. J. Dermatol.* **2007**, *157*, 894–900. [CrossRef] [PubMed]
35. Abuzahra, F.; Spöler, F.; Först, M.; Brans, R.; Erdmann, S.; Merk, H.F.; Obrigkeit, D.H. Pilot study: Optical coherence tomography as a non-invasive diagnostic perspective for real time visualisation of onychomycosis. *Mycoses* **2009**, *53*, 334–339. [CrossRef] [PubMed]
36. Piao, D.; Abreski, D.; Zhu, Q. Preliminary results of imaging and diagnosis of nail fungal infection with optical coherence tomography. In Proceedings of the Biomedical Topical Meeting, Optical Society of America, Miami Beach, FL, USA, 7–10 April 2002; p. SuD5.
37. Sattler, E.; Kaestle, R.; Rothmund, G.; Welzel, J. Confocal laser scanning microscopy, optical coherence tomography and transonychial water loss for in vivo investigation of nails: CLSM, OCT and TOWL for in vivo investigation of nails. *Br. J. Dermatol.* **2012**, *166*, 740–746. [CrossRef]
38. Verne, S.H.; Chen, L.; Shah, V.; Nouri, K.; Tosti, A. Optical Coherence Tomography Features of Dermatophytoma. *JAMA Dermatol.* **2018**, *154*, 225. [CrossRef]
39. Rothmund, G.; Sattler, E.C.; Kaestle, R.; Fischer, C.; Haas, C.J.; Starz, H.; Welzel, J. Confocal laser scanning microscopy as a new valuable tool in the diagnosis of onychomycosis-comparison of six diagnostic methods: Six diagnostic methods for onychomycosis. *Mycoses* **2013**, *56*, 47–55. [CrossRef]
40. Alvarez-Román, R.; Naik, A.; Kalia, Y.N.; Fessi, H.; Guy, R.H. Visualization of skin penetration using confocal laser scanning microscopy. *Eur. J. Pharm. Biopharm.* **2004**, *58*, 301–316. [CrossRef]
41. Shotton, D.; White, N. Confocal scanning microscopy: Three-dimensional biological imaging. *Trends Biochem. Sci.* **1989**, *14*, 435–439. [CrossRef]
42. Cinotti, E.; Fouilloux, B.; Perrot, J.L.; Labeille, B.; Douchet, C.; Cambazard, F. Confocal microscopy for healthy and pathological nail. *J. Eur. Acad. Dermatol. Venereol.* **2014**, *28*, 853–858. [CrossRef]
43. Arrese, J.E.; Quatresooz, P.; Pierard-Franchimont, C.; Pierard, G.E. Nail histomycology. Protean aspects of a human fungal bed. *Ann. Dermatol. Venereol.* **2003**, *130*, 1254–1259.
44. Hongcharu, W.; Dwyer, P.; Gonzalez, S.; Anderson, R.R. Confirmation of onychomycosis by in vivo confocal microscopy. *J. Am. Acad. Dermatol.* **2000**, *42*, 214–216. [CrossRef]

45. Pharaon, M.; Gari-Toussaint, M.; Khemis, A.; Zorzi, K.; Petit, L.; Martel, P.; Baran, R.; Ortonne, J.P.; Passeron, T.; Lacour, J.P.; et al. Diagnosis and treatment monitoring of toenail onychomycosis by reflectance confocal microscopy: Prospective cohort study in 58 patients. *J. Am. Acad. Dermatol.* **2014**, *71*, 56–61. [CrossRef] [PubMed]
46. Gupta, A.K.; Jain, H.C.; Lynde, C.W.; MacDonald, P.; Cooper, E.A.; Summerbell, R.C. Prevalence and epidemiology of onychomycosis in patients visiting physicians' offices: A multicenter Canadian survey of 15,000 patients. *J. Am. Acad. Dermatol.* **2000**, *43*, 244–248. [CrossRef]
47. Feuilhade de Chauvin, M. New diagnostic techniques. *J. Eur. Acad. Dermatol. Venerol.* **2005**, *19*, 20–24. [CrossRef] [PubMed]